Broad Bandgap D–A Copolymer Based on Bithiazole Acceptor Unit for Application in High-Performance Polymer Solar Cells with Lower Fullerene Content

Kun Wang, Xia Guo,* Bing Guo, Wanbin Li, Maojie Zhang,* Yongfang Li*

A new broad bandgap and 2D-conjugated D-A copolymer, **PBDTBTz-T**, based on bithienyl-benzodithiophene donor unit and bithiazole (BTz) acceptor unit, is designed and synthesized for the application as donor material in polymer solar cells (PSCs). The polymer possesses highly coplanar and crystalline structure with a higher hole mobility and lower HOMO energy level which is beneficial to achieve higher open circuit voltage (V_{oc}) of the PSCs with the polymer as donor. The PSCs based on **PBDTBTz-T**:$PC_{71}BM$ blend film with a lower $PC_{71}BM$ content of 40% demonstrate a power conversion efficiency (PCE) of 6.09% with a relatively higher V_{oc} of 0.92 V. These results indicate that the lower HOMO energy level of the BTz-based D–A copolymer is beneficial to a high V_{oc} of the PSCs. The polymer, with highly coplanar and crystalline structure, can effectively reduce the content of fullerene acceptor in the active layer and can enhance the absorption and PCE of the PSCs.

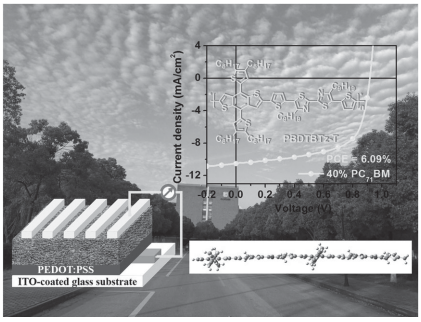

1. Introduction

Over the past decade, bulk-heterojunction polymer solar cells (PSCs) have attracted extensive concern of the researchers because of their advantages of light weight, low cost, easy fabrication, and the capability to be fabricated into flexible large-area devices.[1–8] The studies on PSCs have already made great progress toward higher power conversion efficiency (PCE) in the past five years.[9–22]

PCE of the PSCs is determined by short circuit current density (J_{sc}), open-circuit voltage (V_{oc}), and fill factor (FF) of the devices. Generally, V_{oc} is directly proportional to the offset between the highest occupied molecular orbital (HOMO) level of the donor and the lowest unoccupied molecular orbital (LUMO) level of the acceptor.[23] Therefore, lower HOMO energy level is pursued in the molecular design of the polymer donor materials. On the other hand, broad absorption band (lower bandgap) and higher hole mobilities of the polymer donors with relatively higher LUMO energy level are desirable for realizing higher J_{sc} and FF.[24] However, it is difficult to downshift the HOMO energy level of the low bandgap polymers with remaining relatively higher LUMO energy level for efficient exciton dissociation at the donor/acceptor interfaces. The HOMO energy level of the broad bandgap copolymers is easy to be downshifted for a high $V_{oc.}$ In addition, high

Dr. K. Wang, Prof. X. Guo, B. Guo, W. Li,
Prof. M. Zhang, Prof. Y. Li
Laboratory of Advanced Optoelectronic Materials
College of Chemistry
Chemical Engineering and Materials Science
Soochow University
Suzhou 215123, China
E-mail: guoxia@suda.edu.cn; mjzhang@suda.edu.cn;
liyf@iccas.ac.cn
Prof. Y. Li
Beijing National Laboratory for Molecular Sciences
CAS Key Laboratory of Organic Solids
Institute of Chemistry
Chinese Academy of Sciences
Beijing 100190, China

DOI: 10.1002/marc.201600115

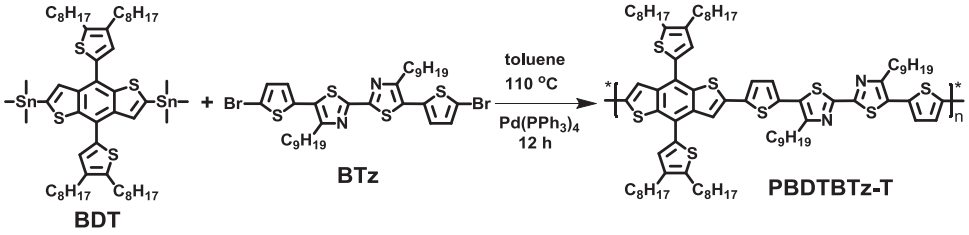

Scheme 1. Synthesis route and molecular structure of **PBDTBTz-T**.

performance broad bandgap polymer donors can be used in tandem PSCs and the nonfullerene PSCs with complementary absorption with low bandgap organic semiconductor acceptors.[25]

Considering that PCBM (an abbreviation of phenyl-C_{61}-butyric acid methyl ester ($PC_{61}BM$) or phenyl-C_{71}-butyricacid methyl ester ($PC_{71}BM$)) usually shows weaker extinction coefficient and narrower absorption bands in visible region than that of the donor photovoltaic materials, hence, the absorption of the active layer could be enhanced by reducing the content of PCBM and increasing the content of polymer donor in the blend film. However, in the active layers of most PSCs, the PCBM content is higher than that of the donor materials.[26–28] Thus, it is an important challenge for molecular design of the polymer donor materials to get high efficiency PSCs with lower fullerene content in the blend active layers.

In 2013, Hou and co-workers achieved an efficient PSCs with high donor:acceptor (D/A) ratio by modifying the substituent position of the alkyl chains in a polythiophene derivative.[29] Sun et al. and our group[30,31] found that the donor materials with highly coplanar and crystalline structure may induce the fullerene acceptor to form percolated pathways in the active layer and hence can form appropriate D/A interpenetrating network with a lower fullerene content.

Bithiazole (BTz)[32–40] is an electron acceptor unit because thiazole contains one electron-withdrawing nitrogen of imine in the place of the carbon atom at the 3-position of thiophene ring. In our previous work,[41–47] we have synthesized a series of D–A copolymers based on BTz as acceptor unit for the photovoltaic application and attained relatively higher PCE. Furthermore, we choose 2D conjugated bithienyl-benzodithiophene (BDT-T) as the donor unit, because of the BDT-T has a symmetric and planar conjugated structure and thus tight and compact stacking can be expected for the BDT-T-based conjugated polymers.[28,48,49]

Based on the above analysis, in this work, we combine BTz acceptor unit and BDT-T donor unit together, to synthesize a new broad bandgap D–A copolymer **PBDTBTz-T** (as shown in Scheme 1), for application as donor material in high-performance PSCs. The polymer shows an absorption in the wavelength range from 300 to 650 nm, lower HOMO energy level, high planarity, high crystallinity, and higher hole mobility. The PCE of the PSCs based on **PBDTBTz-T**/$PC_{71}BM$ with a low $PC_{71}BM$ content of 40% reached 6.09% with a high V_{oc} of 0.92 V. These results indicate that the lower HOMO energy level of the BTz-based D–A copolymer is beneficial to a high V_{oc} of the PSCs. And the highly coplanar and crystalline structure of the polymer donor can effectively reduce the content of fullerene acceptor in the blend active layer, enhance the absorption and PCE of the PSCs.

2. Experimental Section

All chemicals and solvents were reagent grades and purchased from Aldrich, Alfa Aesar, and TCI Chemical Co. Monomers BDT-T and BTz were synthesized according to the procedure reported in the literatures.[32–40] The detailed synthetic processes of the polymer are as follows. The detailed fabrication and characterization of the PSC devices were described in the Supporting Information.

2.1. Synthesis of the Polymer PBDTBTz-T

Monomer BDT-T (565 mg, 0.5 mmol), monomer BTz (371 mg, 0.5 mmol), and dry toluene (15 mL) were added to a 50 mL double-neck round-bottom flask. The reaction container was purged with N_2 for 20 min to remove O_2, and then $Pd(PPh_3)_4$ (20 mg) was added. After another flushing with N_2 for 20 min, the reactant was heated to reflux for 12 h. The reactant was cooled down to room temperature and poured into MeOH (200 mL), and the precipitates were collected by filtration and then washed with MeOH. The solid was dissolved in $CHCl_3$ (100 mL) and passed through a column packed with alumina, Celite, and silica gel. The column was eluted with $CHCl_3$. The combined polymer solution was concentrated and was poured into MeOH. After this, the precipitates were collected and dried under vacuum overnight to get the polymer. Yield: 450 mg (65%). GPC: M_w = 44.0 K; M_n = 22.2 K; M_w/M_n = 1.98.

3. Results and Discussion

3.1. Synthesis and Characterization of the Polymer

The polymer **PBDTBTz-T** was synthesized by Stille coupling reaction as shown in Scheme 1. The ^1H NMR spectra

of polymer **PBDTBTz-T** in $CDCl_3$ was shown in Figure S1 in the Supporting Information. The polymer was purified by silica gel with $CHCl_3$ as eluent. **PBDTBTz-T** possesses good solubility in *o*-dichlorobenzene (*o*-DCB), chlorobenzene, toluene, and chloroform. The molecular weight of the polymer was estimated by high temperature gel-permeation chromatography using 1,2,4-trichlorobenzene as the eluent at 160 °C. The number average molecular weight (M_n) of **PBDTBTz-T** was measured to be 22.2 KDa with a polydispersity index (PDI) of 1.98, as shown in Figure S2 in the Supporting Information. Thermogravimetric analysis was performed to investigate the thermal stability of **PBDTBTz-T** under a N_2 atmosphere. As shown in Figure S5 in the Supporting Information, the onset decomposition temperature of 5% weight-loss at 457 °C for **PBDTBTz-T**, which indicates that the polymer have a high thermal stability for its application in PSCs. Figure S6 in the Supporting Information shows the Differential scanning calorimetry (DSC)(thermograms of **PBDTBTz-T**, there are no apparent endothermic peak and exothermic peak during increasing temperature and decreasing temperature, respectively. The hole mobility of **PBDTBTz-T** is 7.11×10^{-3} cm^2 V^{-1} s^{-1} (as shown in Figure S7 in the Supporting Information), which was measured by the space-charge-limited current method with the device structure of indium tin oxide (ITO)/poly(3,4-ethylenedioxythiophene):poly(styrene sulfonate) (PEDOT:PSS)/**PBDTBTz-T**/Au. Theoretical calculation with density functional theory (DFT) reveals that **PBDTBTz-T** possesses highly coplanar molecular backbone.

3.2. Absorption Spectra and Electronic Energy Levels

As shown in Figure 1a, the absorption spectrum of the polymer film shows an absorption peak at 550 nm, red-shifted by 20 nm compared with that in solution. There is a distinct shoulder peak at 592 nm, indicating strong intermolecular interaction in solid state, which may be ascribed to its larger π-conjugated structure and higher coplanarity. The absorption edge (λ_{edge}) of the polymer film is 655 nm from which the optical bandgap (E_g^{opt}) of the polymer was calculated to be 1.89 eV according to $E_g^{opt} = 1240/\lambda_{edge}$.

The HOMO and LUMO levels of the polymer were determined by the cyclic voltammogram measurement as shown in Figure 1b. The onset oxidation and onset reduction potentials of **PBDTBTz-T** are 0.50 and –1.46 V versus Ag/Ag^+, respectively. According to the equations: HOMO = $-e$ (φ_{ox} + 4.71) (eV), LUMO = $-e$ (φ_{red} + 4.71) (eV),[50–52] the HOMO and the LUMO energy levels of **PBDTBTz-T** are –5.21 and –3.25 eV, respectively. The electrochemical bandgap (E_g^{cv}) of the polymer is 1.96 eV, which is consistent with the optical bandgap calculated from film absorption onset wavelength.

3.3. X-Ray Diffraction Analysis

In order to investigate the crystallinity of **PBDTBTz-T**, we analyzed the X-Ray Diffraction (XRD) profile of pure **PBDTBTz-T** film, as shown in Figure 2. The XRD profile exhibits four diffraction peaks at 2θ = 3.9° (100), 7.8° (200), 11.7° (300), and even 15.6° (400) reflection peaks, respectively, with a *d*-spacing value of 22.6 Å, which corresponds to the interchain distance separated by the alkyl side chains of **PBDTBTz-T**. Moreover, a clear diffraction peak of **PBDTBTz-T** at 2θ = 24.4° (010) was observed, which corresponding to a π–π stacking distance of 3.64 Å, indicating more compact π–π stacking and strong intermolecular interaction between the polymer backbones. The π–π stacking distance of 3.64 Å of **PBDTBTz-T** with BTz as acceptor unit is smaller than most of the other D–A copolymers.[13,15,53–57] The XRD results indicate that **PBDTBTz-T** possesses crystalline structure with ordered polymer chains and densely packed side chains, which is beneficial to realize a higher hole mobility and a better photovoltaic performance of the polymer.

3.4. Theoretical Calculation

Theoretical calculations with DFT at the B3LYP/6-31G(d, p) basis set were performed to predict the energy levels and

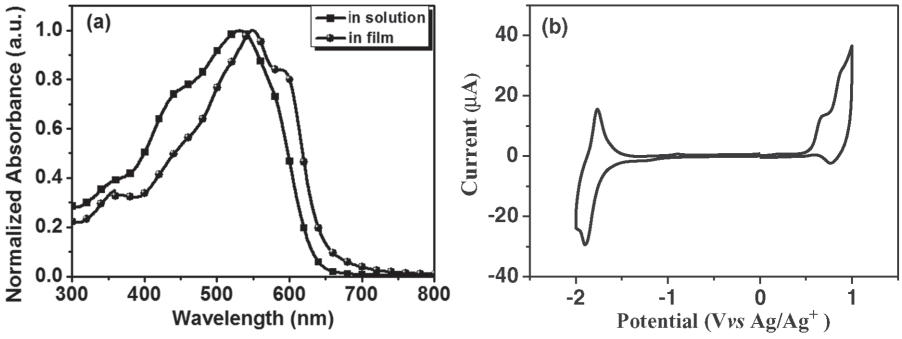

Figure 1. a) UV–vis absorption spectra of **PBDTBTz-T** in chloroform solution and solid film; b) Cyclic voltammogram of **PBDTBTz-T** film on a platinum electrode measured in 0.1 mol L^{-1} Bu_4NPF_6 acetonitrile solution at a scan rate of 50 mV s^{-1}.

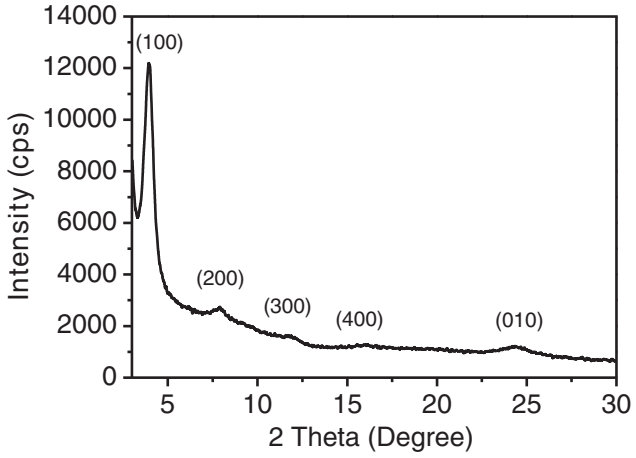

Figure 2. XRD profile of **PBDTBTz-T** film drop-cast from $CHCl_3$ solution onto a Si substrate.

electronic properties of **PBDTBTz-T**. We chose two BDT-BTz repeating units as a simplified model of the molecule to avoid excessive calculation demand, all alkyl side chains in the molecule were also replaced by methyl group to make computation easier. Figure 3 shows the optimized molecular geometries and orbital distribution of HOMO and LUMO of **PBDTBTz-T**. The calculated HOMO and LUMO energy levels of **PBDTBTz-T** are –4.95 and –2.82 eV, respectively. In addition, as can be seen from Figure 3b, the molecular geometry shows a linear molecular skeleton conformation from the side view. And meanwhile, we give the dihedral angles between the BDT unit and the thiophene unit in side chain, as well as the dihedral angles between two adjacent units in the molecular backbone, the corresponding angles are marked in Figure 3c. It is worth noting that the dihedral angle between the two thiazole rings of the BTz units is about 0.2 degree, indicating very good coplanar conformation. The theoretical calculation of the polymer is well consistent with the results in optics and XRD measurement. The molecular orbital distributions (see Figure 3) indicate that the HOMO of **PBDTBTz-T** is delocalized along the whole π-conjugated backbone of the molecule while its LUMO is mainly localized on its BTz-based acceptor segment.

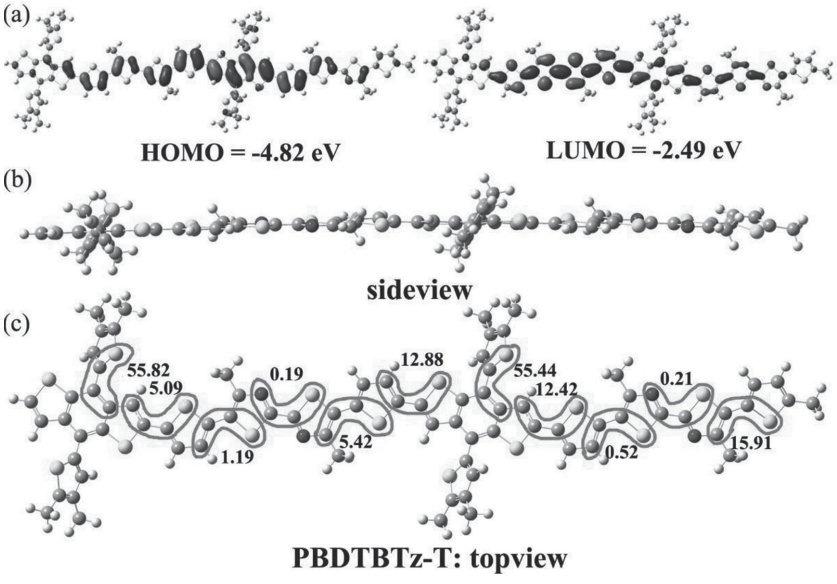

Figure 3. a) The frontier molecular orbital of **PBDTBTz-T** obtained from DFT calculations at the B3LYP/6-31G (d, p) level, (left) HOMO energy level, (right) LUMO energy level; b) the molecular plane by side view; c) calculated dihedral angles between the thiophene unit in side chain and the BDT unit, as well as the dihedral angles between two adjacent unit in the molecular backbone.

3.5. Photovoltaic Properties

The photovoltaic properties of **PBDTBTz-T** were studied by fabricating the PSCs with a traditional device structure of ITO/ PEDOT:PSS/active layer/Ca (20 nm)/Al (80 nm). The active layers with **PBDTBTz-T** as donor and $PC_{71}BM$ as acceptor were spin-coated from *o*-DCB blend solution of **PBDTBTz-T** and $PC_{71}BM$. Figure 4 shows the current density–voltage (*J–V*) characteristics, external quantum efficiency (EQE) of the optimized PSCs and the UV–vis absorption spectra of **PBDTBTz-T**:$PC_{71}BM$ blend films with different donor/acceptor (D/A) weight ratios, and the relevant photovoltaic parameters were collected in Table 1 for a clear comparison.

The PSCs based on **PBDTBTz-T**:$PC_{71}BM$ (1:1.5, w/w) with the $PC_{71}BM$ content of 60% showed a PCE of 3.99% with a V_{oc} of 0.93 V, J_{sc} of 8.56 mA cm^{-2}, and a FF of 50.0% (Table S3, Supporting Information). When the D/A weight ratio of the blend film increased to 1:1 where the $PC_{71}BM$ content is decreased to 50%, the device demonstrated a PCE of 5.32% with a V_{oc} of 0.91 V, J_{sc} of 9.51 mA cm^{-2}, and a FF of 61.5%. The PCE of the PSCs improved to 6.09% when the D/A ratio increased to 1.5:1 (the $PC_{71}BM$ content is decreased to 40%), with a V_{oc} of 0.92 V, J_{sc} of 10.53 mA cm^{-2}, and a FF of 62.9%. Further decreasing the content of $PC_{71}BM$ to 33% (D/A ratio of 2:1), the PCE of the PSCs declined to 4.96%, due to the decreased FF of the device. To the best of our knowledge, PSCs with the D/A weight ratio of 1.5:1 for our new broad bandgap D–A copolymer **PBDTBTz-T** is one of the lowest optimized content of fullerene acceptor (40%) in PSCs reported in literature so far.[29] In addition, the PCE of 6.09% was achieved without any extra treatment such as thermal annealing, solvent additives, solvent annealing, etc. The broad bandgap polymer **PBDTBTz-T**

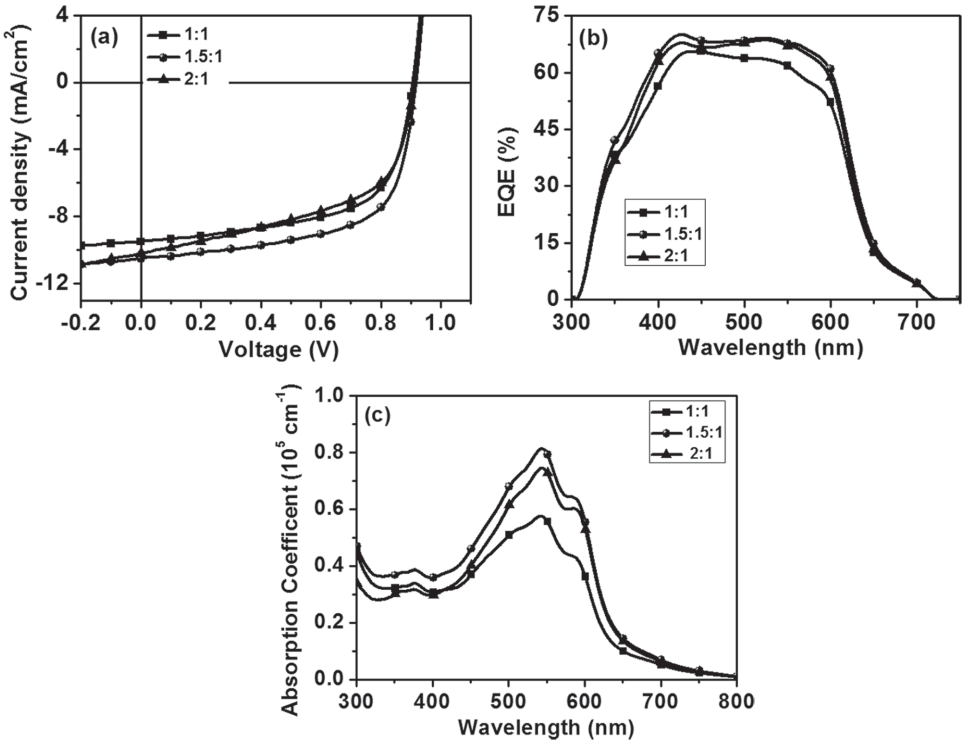

Figure 4. a) *J–V* characteristics; b) EQE curves of the PSCs based on **PBDTBTz-T**:$PC_{71}BM$ blend film with different D/A weight ratios; c) UV–vis absorption spectra of the blend active layers of the corresponding devices.

with good photovoltaic performance could be used in tandem PSCs or nonfullerene PSCs with narrow bandgap n-type organic semiconductor as acceptor for the complementary absorption in Vis–NIR region. And facilitate the large scale roll-to-roll production in future applications.

We investigated the effect of the thermal annealing and solvent additives on the photovoltaic performance of the PSCs with the D/A weight ratio of 1.5:1. However, the treatment of both the thermal annealing and solvent additives results in slight decrease of the PCE of the devices, due mainly to the decrease of FF. The corresponding *J–V* curves and the photovoltaic parameters of the PSCs with different treatments are shown in Figures S8, S9 and Tables S1, S2 in the Supporting Information.

In order to investigate the effect of the polymer molecular weight on the photovoltaic performance of the PSCs as the molecular weight of the donor is greatly affecting the device efficiency. Other batches of **PBTTTz-T**, namely **PBTTTz-T (2),** and **PBTTTz-T (3)** were synthesized by Stille coupling reaction according to Carothers' equation. The M_n values of **PBDTBTz-T (2)** and **PBDTBTz-T (3)** were measured to be 16.0 and 18.1 KDa with a PDI of 1.81 and 1.72, respectively (see Figures S3, S4 in the Supporting Information). The photovoltaic parameters of the PSCs based on **PBDTBTz-T (2)** or **PBDTBTz-T (3)**:$PC_{71}BM$ with different conditions are shown in Figures S10, S11 and Tables S3, S4 in the Supporting Information. The results indicate that the polymer with lower molecular weight show slightly decreased photovoltaic performance, mainly due to the decreased FF of the PSCs, which is consistent with the literature reports.[58,59]

In addition, although the photovoltaic performance of the **PBDTBTz-T**-based PSCs is lower than that of the BDT-based narrow bandgap 2D conjugated polymers[9,11,49] due to the lower J_{sc} and FF because of the narrower absorbption in the ultraviolet visible range, the narrow bandgap conjugated polymers with higher HOMO energy level are limited for realizing higher V_{oc}. As is well known, the photovoltaic performance of the D-A copolymer donor materials are closely related to the acceptor units in the D-A

Table 1. Photovoltaic performance parameters of the PSCs based on **PBTTTz-T** as donor and $PC_{71}BM$ as acceptor with different D/A weight ratios under illumination of AM 1.5 G, 100 mW cm^{-2}.

D/A ratio	V_{oc} [V]	J_{sc} [mA cm^{-2}]	J_{sc} [mA cm^{-2}][a)]	FF [%]	PCE [%][b)]
1:1	0.91	9.51	9.05	61.5	5.32 ± 0.10
1.5:1	0.92	10.53	10.11	62.9	6.09 ± 0.06
2:1	0.91	10.20	9.70	53.4	4.96 ± 0.15

[a)]Integrated from EQE; [b)]The values are the device average PCEs and their standard deviation based on more than 10 devices.

copolymers. Actually, the polymer **PBDTBTz-T** shows a relatively desirable photovoltaic performance without any extra treatment in the D-A copolymers based on BTz acceptor unit.[32–47]

The EQE curves and the UV–vis absorption spectra of the devices with different D/A weight ratios are shown in Figure 4b,c, respectively. And the corresponding integral current density values from EQE are listed in Table 1. When 50% $PC_{71}BM$ was used (D/A ratio of 1:1), the active layer showed a low absorption, because $PC_{71}BM$ possesses a weaker extinction coefficient in visible region, so the device showed a relatively low EQE over the whole response range. When the $PC_{71}BM$ content was reduced to 40% (D/A ratio of 1.5:1), the active layer showed strong absorption, the EQE of the device enhanced obviously, and thus a higher integral current of 10.11 mA cm^{-2} was obtained. Meanwhile, the FF of the device improved slightly, and consequently the PCE reached 6.09%. When further decreasing the content of $PC_{71}BM$, the absorbance at 300–650 nm obviously dropped, as a result, the EQE and FF dramatically decreased. Furthermore, it is noteworthy that the current densities calculated from the EQE curves under the standard solar spectrum (AM 1.5G) are consistent with the J_{sc} values obtained from the *J–V* measurement with deviation less than 5%, indicating that the *J–V* measurements in this work are reliable.

3.6. Grazing Incidence X-Ray Diffraction Study

To gain a deeper insight into the crystallinity and molecular stacking mode of **PBDTBTz-T** in the active layer, grazing incidence X-ray diffraction (GIXD) measurements were carried out to investigate molecular packing of the pure **PBDTBTz-T** film and the blend film of **PBDTBTz-T** and $PC_{71}BM$. Figure 5 shows 2D GIXD images and the corresponding profiles of the samples, including thin film for pure **PBDTBTz-T** and the **PBDTBTz-T**/$PC_{71}BM$ blend films with different conditions, which were cast from *o*-DCB. For the pure **PBDTBTz-T** film, as shown in Figure 5a,a′, the out-of-plane profile shows pronounced 100, 200, 300, and 400 diffraction peaks at 0.27, 0.54, 0.81, and 1.08 $Å^{-1}$, respectively, arising from the alkyl chain packing with *d*-spacing of ≈22.6 Å. Moreover, the out-of-plane of pure **PBDTBTz-T** film shows an intensive and sharp peak at 1.72 $Å^{-1}$ (010), which corresponds to the π–π stacking with a *d*-spacing of 3.64 Å. However, the in-plane profile of pure **PBDTBTz-T** film shows only a sharp peak at 0.27 $Å^{-1}$ (010). The result indicates that the pure **PBDTBTz-T** film exhibits a face on dominated molecular orientation with respect to the substrate. When blended with $PC_{71}BM$, the crystalline structure of the polymer is well maintained both in out-of-plane and in-plane accompanying the appearance of a broad diffraction peak at ≈1.33 $Å^{-1}$, which is attributed to $PC_{71}BM$ aggregation (see Figure 5b–e and 5b′–e′). It is worth noting that when the blend film with D/A ratio of 1.5:1 was treated by thermal annealing at 100 °C for 10 min, the lamellar diffraction and π–π stacking diffraction significantly increased. The GIXD results are consistent with the optimized photovoltaic performance.

3.7. Morphology Study

Transmission electron microscopy (TEM) and tapping-mode atomic force microscopy (AFM) were used to investigate the bulk and surface morphologies of the active layers prepared with different conditions. Figure 6 shows the TEM images of the active layers of the PSCs. As we can see

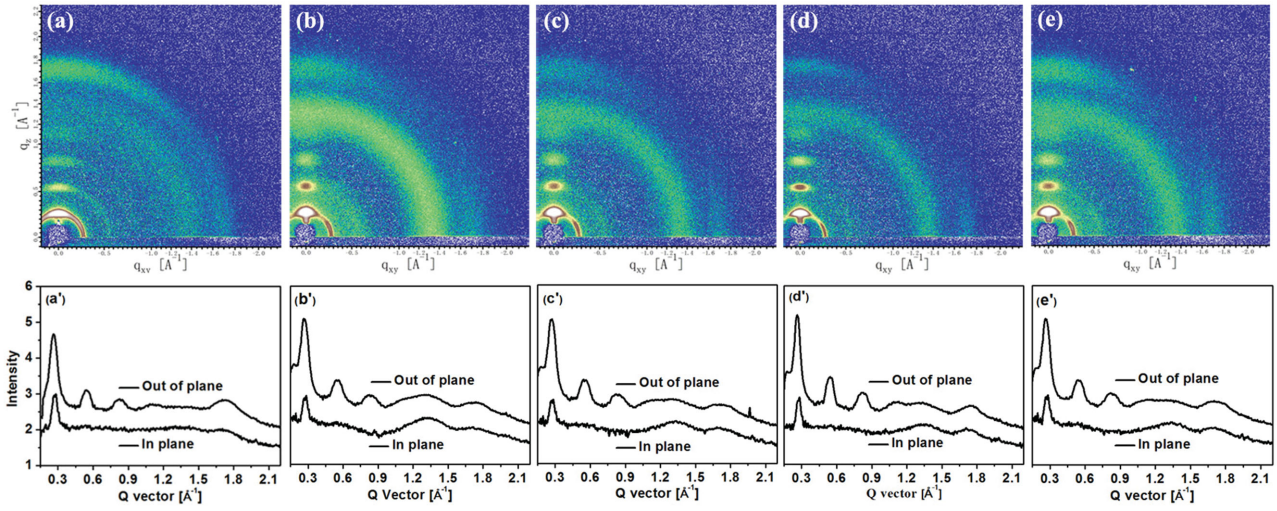

Figure 5. 2D GIXD images and the corresponding profiles of the pure **PBDTBTz-T** film and **PBDTBTz-T**/$PC_{71}BM$ blend films with different conditions. (a) and (a′): pure **PBDTBTz-T** film; (b) and (b′): blend film with D/A = 1:1; (c) and (c′): blend film with D/A = 1.5:1; (d) and (d′): blend film with D/A = 1.5:1, 100 °C thermal annealing for 10 min; (e) and (e′): blend film with D/A = 2:1

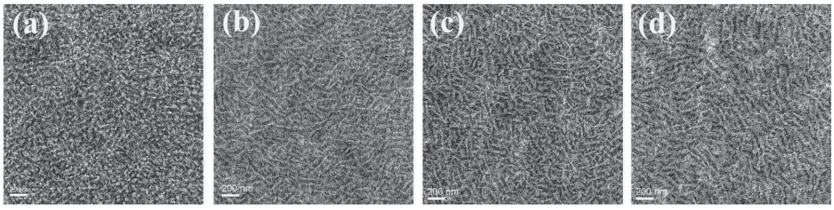

Figure 6. TEM images of **PBDTBTz-T**:$PC_{71}BM$ blend films with different D/A weight ratios. a) 1:1; b) 1.5:1; c) 1.5:1 with 100 °C annealing for 10 min; d) 2:1.

in Figure 6a, large-scale phase-separated morphology can be clearly seen in the TEM image for the blend film with $PC_{71}BM$ content of 50%, which may cause more geminate and bimolecular recombination and result in lower J_{sc} of the PSCs. When the $PC_{71}BM$ content was decreased to 40% (D/A ratio of 1.5:1), an appropriate D/A febril interpenetrating network was observed with size of ≈20–30 nm (as shown in Figure 6b), which is beneficial for charge separation and transport, and thus a high J_{sc} and FF of the device were obtained. The TEM results are consistent with the optimized photovoltaic performance. When the active layer was treated by thermal annealing at 100 °C for 10 min or further decreasing the $PC_{71}BM$ content (D/A ratio of 2:1), although the clear interpenetrating network can be seen (Figure 6c,d), the fiber diameters of the network were increased to a large size. The too large aggregation could lead to the decreasing FF for the PSCs with thermal treatment and the device with D/A weight ratio of 2:1.

AFM images of the blends film with different treatment conditions are shown in Figure S12 in the Supporting Information. In the blend films with 50% and 40% $PC_{71}BM$ content, the root-mean-square roughness (R_q) of the blend films are 2.25, 3.15, and 3.76 nm (with thermal annealing at 100 °C for 10 min), respectively (as shown in Figure S12a–c, S12e–g in the Supporting Information). The R_q of the blend film increased to 4.5 nm when the $PC_{71}BM$ content decreased to 33% (see Figure S12d,h in the Supporting Information). The increased R_q is attributed to the enhanced crystallization of **PBDTBTz-T** with the increase of donor content in the blend film. Furthermore, as we can see in Figure S12i–l in the Supporting Information, suitable phase separation was formed in the active layers with the $PC_{71}BM$ content of 50% and 40%, and thus a relatively high FF was obtained. Further increasing the D/A ratio to 2:1 or treating by thermal annealing, a large phase separation size of the blend film was formed, leading to the FF dramatically decreased. The AFM results are consistent with the TEM results, GIXD results, and the optimized photovoltaic performance.

4. Conclusions

In summary, a new 2D-conjugated and broad bandgap D–A copolymer, **PBDTBTz-T**, based on BDT-T donor unit and BTz acceptor unit, was designed and synthesized for the application as donor material in PSCs. The polymer shows an absorption in the wavelength range from 300 to 650 nm, and possesses highly planar and crystalline structure and higher hole mobility. A PCE of 6.09% was obtained for the PSCs with the polymer as donor and with a low $PC_{71}BM$ acceptor content of 40% in the active layer. These results indicate that the lower HOMO energy level of the BTz-based D–A copolymer is beneficial to a high V_{oc} of the PSCs. And the polymer with highly coplanar and crystalline structure can effectively reduce the content of fullerene acceptor in the active layer, so as to enhance the absorption and PCE of the PSCs.

Supporting Information

Supporting Information is available from the Wiley Online Library or from the author.

Acknowledgements: This work was supported by the National Natural Science Foundation of China (NSFC) (Grant Nos. 91333204, 51203168, 51422306, 51503135, 51573120, and 201502134), the Priority Academic Program Development of Jiangsu Higher Education Institutions, the Jiangsu Provincial Natural Science Foundation (Grant No. BK20150332), the Natural Science Foundation of the Jiangsu Higher Education Institutions of China (Grant No. 15KJB430027).

Received: February 23, 2016; Revised: April 22, 2016; Published online: May 13, 2016; DOI: 10.1002/marc.201600115

Keywords: 2D-conjugated D–A copolymers; bithiazole (BTz) acceptor units; bithienyl-benzodithiophenes; low fullerene content; polymer solar cells

[1] G. Yu, J. Gao, J. C. Hummelen, F. Wudl, A. J. Heeger, *Science* **1995**, *270*, 1789.
[2] S. Günes, H. Neugebauer, N. S. Sariciftci, *Chem. Rev.* **2007**, *107*, 1324.
[3] L. Lu, T. Zheng, Q. Wu, A. M. Schneider, D. Zhao, L. Yu, *Chem. Rev.* **2015**, *115*, 12666.
[4] Y. F. Li, *Acc. Chem. Res.* **2012**, *45*, 723.
[5] Z. G. Zhang, Y. F. Li, *Sci. China Chem.* **2015**, *58*, 192.
[6] K. R. Graham, C. Cabanetos, J. P. Jahnke, M. N. Idso, A. E. Labban, G. O. N. Ndjawa, T. Heumueller, K. Vandewal, A. Salleo, B. F. Chmelka, A. Amassian, P. M. Beaujuge, M. D. McGehee, *J. Am. Chem. Soc.* **2014**, *136*, 9608.
[7] J. D. Chen, C. H. Cui, Y. Q. Li, L. Zhou, Q. D. Ou, C. Li, Y. F. Li, J. X. Tang, *Adv. Mater.* **2015**, *27*, 1035.
[8] F. C. Krebs, *Sol. Energy Mater. Sol. Cells* **2009**, *93*, 394.
[9] a) C. H. Cui, W.-Y. Wong, Y. F. Li, *Energy Environ. Sci.* **2014**, *7*, 2276; b) C. H. Cui, Z. C. He, Y. Wu, X. Cheng, H. B. Wu, Y. F. Li, Y. Cao, W.-Y. Wong, *Energy Environ. Sci.* **2016**, *9*, 885.
[10] Z. He, B. Xiao, F. Liu, H. Wu, Y. Yang, S. Xiao, C. Wang, T. P. Russell, Y. Cao, *Nat. Photonics* **2015**, *9*, 174.

[11] S.-H. Liao, H.-J. Jhuo, Y.-S. Cheng, S.-A. Chen, *Adv. Mater.* **2013**, *25*, 4766.
[12] J. You, L. Dou, K. Yoshimura, T. Kato, K. Ohya, T. Moriarty, K. Emery, C.-C. Chen, J. Gao, G. Li, Y. Yang, *Nat. Commun.* **2013**, *4*, 1446.
[13] a) M. Zhang, Y. Gu, X. Guo, F. Liu, S. Zhang, L. Huo, T. P. Russell, J. Hou. *Adv. Mater.* **2013**, *25*, 4944; b) M. Zhang, X. Guo, W. Ma, S. Zhang, L. Huo, H. Ade, J. Hou, *Adv. Mater.* **2014**, *26*, 2089.
[14] S. Zhang, L. Ye, W. Zhao, B. Yang, Q. Wang, J. H. Hou. *Sci. China Chem.* **2015**, *58*, 248.
[15] Y. Liu, J. Zhao, Z. Li, C. Mu, W. Ma, H. Hu, K. Jiang, H. Lin, H. Ade, H. Yan, *Nat. Common.* **2014**, *5*, 5293.
[16] S. Nam, J. Seo, S. Woo, W. H. Kim, H. Kim, D. D. C. Bradley, Y. Kim, *Nat. Commun.* **2015**, *6*, 8929.
[17] N. Zhou, X. Guo, R. P. Ortiz, T. Harschneck, E. F. Manley, S. J. Lou, P. E. Hartnett, X. Yu, N. E. Horwitz, P. M. Burrezo, T. J. Aldrich, J. T. L. Navarrete, M. R. Wasielewski, L. X. Chen, R. P. H. Chang, A. Facchetti, T. J. Marks, *J. Am. Chem. Soc.* **2015**, *137*, 12565.
[18] K. Kawashima, Y. Tamai, H. Ohkita, I. Osaka, K. Takimiya, *Nat. Commun.* **2015**, *6*, 10085.
[19] V. Vohra, K. Kawashima, T. Kakara, T. Koganezawa, I. Osaka, K. Takimiya, H. Murata, *Nat. Photonics* **2015**, *9*, 403.
[20] T. Kim, J.-H. Kim, T. E. Kang, C. Lee, H. Kang, M. Shin, C. Wang, B. Ma, U. Jeong, T.-S. Kim, B. J. Kim, *Nat. Commun.* **2015**, *6*, 8547.
[21] L. Lu, M. A. Kelly, W. You, L. Yu, *Nat. Photonics* **2015**, *9*, 491.
[22] K. A. Mazzio, C. K. Luscombe, *Chem. Soc. Rev.* **2015**, *44*, 78.
[23] M. C. Scharber, D. Mühlbacher, M. Koppe, P. Denk, C. Waldauf, A. J. Heeger, C. J. Brabec, *Adv. Mater.* **2006**, *18*, 789.
[24] a) H. Choi, S.-J. Ko, T. Kim, P.-O. Morin, B. Walker, B. H. Lee, M. Leclerc, J. Y. Kim, A. J. Heeger, *Adv. Mater.* **2015**, *27*, 3318; b) C. M. Proctor, J. A. Love, T.-Q. Nguyen, *Adv. Mater.* **2014**, *26*, 5957; c) W. Li, K. H. Hendriks, W. S. C. Roelofs, Y. Kim, M. M. Wienk, R. A. J. Janssen, *Adv. Mater.* **2013**, *25*, 3182.
[25] a) L. Gao, Z.-G. Zhang, L. Xue, J. Min, J. Zhang, Z. Wei, Y. F. Li, *Adv. Mater.* **2016**, *28*, 1884; b) H. Lin, S. Chen, Z. Li, J. Y. L. Lai, G. Yang, T. McAfee, K. Jiang, Y. Li, Y. Liu, H. Hu, J. Zhao, W. Ma, H. Ade, H. Yan, *Adv. Mater.* **2015**, *27*, 7299; c) H. J. Bin, Z.-G. Zhang, L. Gao, S. S. Chen, L. Zhong, L. W. Xue, C. Yang, Y. F. Li, *J. Am. Chem. Soc.* **2016**, *138*, 4657.
[26] H. Chen, J. Hou, S. Zhang, Y. Liang, G. Yang, Y. Yang, L. Yu, Y. Wu, G. Li, *Nat. Photonics* **2009**, *3*, 649.
[27] a) R. Po, G. Bianchi, C. Carbonera, A. Pellegrino, *Macromolecules* **2015**, *48*, 453; b) K. Wang, B. Guo, W. Su, X. Guo, M. Zhang, Y. Li, *RSC Adv.* **2016**, *6*, 14229.
[28] L. Ye, S. Zhang, L. Huo, M. Zhang, J. Hou, *Acc. Chem. Res.* **2014**, *47*, 1595.
[29] D. Qian, W. Ma, Z. Li, X. Guo, S. Zhang, L. Ye, H. Ade, Z. Tan, J. Hou, *J. Am. Chem. Soc.* **2013**, *135*, 8464.
[30] Y. Sun, G. C. Welch, W. Leong, C. J. Takacs, G. C. Bazan, A. J. Heeger, *Nat. Mater.* **2011**, *11*, 44.
[31] K. Wang, B. Guo, Z. Xu, X. Guo, M. Zhang, Y. Li, *ACS Appl. Mater. Interfaces* **2015**, *7*, 24686.
[32] W.-Y. Wong, X.-Z. Wang, Z. He, K.-K. Chan, A. B. Djurišić, K.-Y. Cheung, C.-T. Yip, A. M.-C. Ng, Y. Y. Xi, C. S. K. Mak, W.-K. Chan, *J. Am. Chem. Soc.* **2007**, *129*, 14372.
[33] H. Wang, Q. Shi, Y. Lin, H. Fan, P. Cheng, X. Zhan, Y. Li, D. Zhu, *Macromolecules* **2011**, *44*, 4213.
[34] P. Bujak, I. Kulszewicz-Bajer, M. Zagorska, V. Maurel, I. Wielgus, A. Pron, *Chem. Soc. Rev.* **2013**, *42*, 8895.
[35] Y. Lin, H. Fan, Y. Li, X. Zhan, *Adv. Mater.* **2012**, *24*, 3087.
[36] D. H. Kim, H.-J. Shin, H. S. Lee, J. Lee, B.-L. Lee, W. H. Lee, J.-H. Lee, K. Cho, W.-J. Kim, S. Y. Lee, J.-Y. Choi, J. M. Kim, *ACS Nano* **2014**, *6*, 662.
[37] B. Fu, C.-Y. Wang, B. D. Rose, Y. Jiang, M. Chang, P.-H. Chu, Z. Yuan, C. Fuentes-Hernandez, B. Kippelen, J.-L. Brédas, D. M. Collard, E. Reichmanis, *Chem. Mater.* **2015**, *27*, 2928.
[38] a) M. Kuramochi, J. Kuwabara, W. Lu, T. Kanbara, *Macromolecules* **2014**, *47*, 7378; b) W. Lu, J. Kuwabara, M. Kuramochi, T. Kanbara, *J. Polym. Sci. A: Polym. Chem.* **2015**, *53*, 1396.
[39] H. Usta, W. C. Sheets, M. Denti, G. Generali, R. Capelli, S. Lu, X. Yu, M. Muccini, A. Facchetti, *Chem. Mater.* **2014**, *26*, 6542.
[40] X. Guo, J. Quinn, Z. Chen, H. Usta, Y. Zheng, Y. Xia, J. W. Hennek, R. P. Ortiz, T. J. Marks, A. Facchetti, *J. Am. Chem. Soc.* **2013**, *135*, 1986.
[41] M. Zhang, H. Fan, X. Guo, Y. He, Z.-G. Zhang, J. Min, J. Zhang, G. Zhao, X. Zhan, Y. Li, *Macromolecules* **2010**, *43*, 8714.
[42] M. Yang, B. Peng, B. Liu, Y. Zou, K. Zhou, Y. He, C. Pan, Y. Li, *J. Phys. Chem. C* **2010**, *114*, 17989.
[43] M. Zhang, X. Guo, Y. Li, *Adv. Energy Mater.* **2011**, *1*, 557.
[44] M. Zhang, X. Guo, X. Wang, H. Wang, Y. Li, *Chem. Mater.* **2011**, *23*, 4264.
[45] M. Zhang, Y. Sun, X. Guo, C. Cui, Y. He, Y. Li, *Macromolecules* **2011**, *44*, 7625.
[46] M. Zhang, X. Guo, Y. Li, *Macromolecules* **2011**, *44*, 8798.
[47] X. Guo, M. Zhang, L. Huo, C. Cui, Y. Wu, J. Hou, Y. Li, *Macromolecules* **2012**, *45*, 6930.
[48] L. Huo, J. Hou, S. Zhang, H.-Y. Chen, Y. Yang, *Angew. Chem. Int. Ed.* **2010**, *49*, 1500.
[49] L. Huo, S. Zhang, X. Guo, F. Xu, Y. Li, J. Hou, *Angew. Chem. Int. Ed.* **2011**, *50*, 9697.
[50] Y. Li, Y. Cao, J. Gao, D. Wang, G. Yu, A. J. Heeger, *Synth. Met.* **1999**, *99*, 243.
[51] Q. Sun, H. Wang, C. Yang, Y. Li, *J. Mater. Chem.* **2003**, *13*, 800.
[52] C. M. Cardona, W. Li, A. E. Kaifer, D. Stockdale, G. C. Bazan, *Adv. Mater.* **2011**, *23*, 2367.
[53] D. H. Kim, B.-L. Lee, H. Moon, H. M. Kang, E. J. Jeong, J.-I. Park, K.-M. Han, S. Lee, B. W. Yoo, B. W. Koo, J. Y. Kim, W. H. Lee, K. Cho, H. A. Becerril, Z. Bao, *J. Am. Chem. Soc.* **2009**, *131*, 6124.
[54] Y. Liu, H. Dong, S. Jiang, G. Zhao, Q. Shi, J. Tan, L. Jiang, W. Hu, X. Zhan, *Chem. Mater.* **2013**, *25*, 2649.
[55] J. Lee, J. W. Chung, J. Jang, D. H. Kim, J.-I. Park, E. Lee, B.-L. Lee, J.-Y. Kim, J. Y. Jung, J. S. Park, B. Koo, Y. W. Jin, D. H. Kim, *Chem. Mater.* **2013**, *25*, 1927.
[56] H. Hu, K. Jiang, G. Yang, J. Liu, Z. Li, H. Lin, Y. Liu, J. Zhao, J. Zhang, F. Huang, Y. Qu, W. Ma, H. Yan, *J. Am. Chem. Soc.* **2015**, *137*, 14149.
[57] J. Zhao, Y. Li, A. Hunt, J. Zhang, H. Yao, Z. Li, J. Zhang, F. Huang, H. Ade, H. Yan, *Adv. Mater.* **2015**, *28*, 1868.
[58] T.-Y. Chu, J. Lu, S. Beaupré, Y. Zhang, J.-R. Pouliot, J. Zhou, A. Najari, M. Leclerc, Y. Tao, *Adv. Funct. Mater.* **2015**, *22*, 2345.
[59] H. Kang, M. A. Uddin, C. Lee, K.-H. Kim, T. L. Nguyen, W. Lee, Y. Li, C. Wang, H. Y. Woo, B. J. Kim, *J. Am. Chem. Soc.* **2015**, *137*, 2359.